# Calcium Binding Induces Interaction between the N- and C-Terminal Domains of Yeast Calmodulin and Modulates Its Overall Conformation†

Ken-ichi Nakashima,‡ Hiroaki Ishida,§ Shin-ya Ohki,§,|| Kunio Hikichi,§ and Michio Yazawa*,‡

*Divisions of Chemistry and Biological Sciences, Graduate School of Science, Hokkaido University, Sapporo 060-0810, Japan*

*Received August 25, 1998; Revised Manuscript Received October 26, 1998*

ABSTRACT: Calmodulin from the yeast *Saccharomyces cerevisiae* binds 3 mol of $Ca^{2+}$ cooperatively. We report here lines of evidence supporting the intramolecular interaction between the N- and C-terminal domains which modulates the $Ca^{2+}$ binding properties of yeast calmodulin. First, the sum of the $Ca^{2+}$ binding curves of the N-terminal and the C-terminal half-molecule did not yield the $Ca^{2+}$ binding curve of yeast calmodulin. Second, the mean residue CD of yeast calmodulin at 222 nm ($-\Delta\epsilon_{222}$) decreased with increases in the concentration of $Ca^{2+}$, whereas those of each half-molecule increased. Finally, the C2 proton of His107 in the C-terminal domain of yeast calmodulin showed three resonance peaks with increases in the concentration of $Ca^{2+}$, each corresponding to the apo, the intermediate, and the $Ca^{2+}$-saturated state. The intermediate peak could not be observed in the C-terminal half-molecule of yeast calmodulin. Computer simulation considering the macroscopic $Ca^{2+}$ binding constants assigned this intermediate to a species consisting of the apo C-terminal domain and the N-terminal domain with at least one of the two sites occupied by $Ca^{2+}$. Peptide segments spanning the defective fourth $Ca^{2+}$ binding site may be involved in the interdomain interaction and the yeast-specific function of calmodulin.

Calmodulin (CaM)[1] is a ubiquitous $Ca^{2+}$ binding protein which modulates many intracellular $Ca^{2+}$-dependent processes. Primary structures of CaMs from various sources consist of the four $Ca^{2+}$ binding sites of the EF-hand motif (*1*), and they are highly conserved among all eukaryotes except the one from baker's yeast, *Saccharomyces cerevisiae* (*2*, *3*). Yeast CaM exhibits only about 60% identity in the primary structure compared to vertebrate CaM (*4*, *5*), binds only 3 mol of $Ca^{2+}$ because of the divergent structure of the fourth $Ca^{2+}$ binding site (site IV, the most C-terminal $Ca^{2+}$ binding site) (*6*), and can activate very poorly the target enzymes from vertebrates (*6*, *7*). Because these properties are different from those of other CaMs, mutational effects of yeast CaM have been studied with an aim to understanding the mechanism of target activation (*5*, *8*−*11*). Since CaM is essential in yeast (*4*, *12*), the characteristic structure of yeast CaM would be essential for the interaction with specific targets in yeast cells.

Recent structural analyses by NMR and X-ray crystallography offered a structural basis for the $Ca^{2+}$-dependent activation process of target proteins by CaM (reviewed in ref *13*). CaM consists of the N- and C-terminal half-molecular domain connected by a flexible helical linker. Each domain contains two $Ca^{2+}$ binding sites and flickers in an independent manner (*14*, *15*). In the $Ca^{2+}$-saturated form, each domain exposes a hydrophobic core with many Met residues on the molecular surface (*16*), while they are buried in the molecular inside in the apo form (*17*, *18*). In the process of target recognition, the exposed hydrophobic residues play a critical role in binding to targets (*19*−*21*).

Earlier biochemical studies involving limited tryptic digestion (*22*, *23*) showed these features of CaM (*24*−*27*). Similar biochemical studies and NMR measurements with yeast CaM (*28*−*30*) suggested a conformational similarity between yeast and vertebrate CaM.

On the other hand, it has been reported that yeast and vertebrate CaMs have different properties. The $Ca^{2+}$ dependence of the CD spectral change of yeast CaM was different from the one of vertebrate CaM (*5*, *7*). Measurements of small-angle X-ray scattering did not suggest a typical dumbbell shape for yeast CaM in solution (*31*). Tryptic digestion of yeast CaM showed cleavage at R126, while vertebrate CaM was preferentially cut at the central linker in the presence of $Ca^{2+}$ (*22*, *23*, *28*). Binding of three $Ca^{2+}$ to yeast CaM is highly cooperative; vertebrate CaM binds a pair of $Ca^{2+}$ to each of the apparently independent half-molecular domains (*6*, *11*, *29*), and a possible interaction between the two domains of yeast CaM has been suggested from the NMR measurements (*29*). Studies on chimeric proteins of yeast and chicken CaM suggested some role of the C-terminal region of yeast CaM, giving a strong cooperativity among all three $Ca^{2+}$ binding sites (*11*).

† This work was supported in part by a Grant-in-Aid for Scientific Research (07309013) from the Ministry of Education, Science and Culture of Japan.

* Address for correspondence: Division of Chemistry, Graduate School of Science, Hokkaido University, Sapporo 060-0810, Japan. Fax: 81-11-706-4924. E-mail: myazawa@sci.hokudai.ac.jp.

‡ Division of Chemistry.

§ Division of Biological Sciences.

|| Present address: Department of Chemistry, Faculty of Science, Tokyo Metropolitan University, Hachioji, Tokyo 192-0364, Japan.

[1] Abbreviations: CaM, calmodulin; CD, circular dichroism; F12 and F34, N- and C-terminal half-molecular fragment, respectively, of scallop CaM prepared by tryptic digestion; MOPS, 3-(*N*-morpholino)propanesulfonic acid; PAGE, polyacrylamide gel electrophoresis; TCA, trichloroacetic acid; Y12, N-terminal half-molecular domain of yeast CaM expressed in *E. coli*, formerly named YCM0N; Y34, C-terminal half-molecular domain of yeast CaM; YCMΔ, yeast CaM mutant protein formerly named YCMΔ132−148.

10.1021/bi982067t CCC: $18.00 
Published on Web 12/15/1998

Here we generated the recombinant proteins corresponding to the two half-molecular domains (Y12 and Y34) of yeast CaM and compared their $Ca^{2+}$ binding properties with those of YCMΔ (*5*) and the tryptic fragments, F12 and F34, of scallop CaM (*25*) as well as with those of yeast and vertebrate CaM. The region in yeast CaM corresponding to the C-terminal $Ca^{2+}$ binding site (site IV) of vertebrate CaM was revealed to be involved in the $Ca^{2+}$-dependent interdomain interaction and may play a specific role in the CaM-dependent regulation in yeast cells.

## MATERIALS AND METHODS

*Protein Engineering.* An *Escherichia coli* expression plasmid encoding the C-terminal half domain (Y34) of yeast CaM (YCM0) was constructed as follows. Two restriction sites for *Nco*I were generated by site-directed mutagenesis in plasmid pY encoding YCM0 (*5*) in a manner similar to that reported previously (*11*). The first site was created at the initiation codon, and the other site was at a region encoding Leu69. The constructed plasmid pY(*Nco*I-1/70) was digested with *Nco*I, and the products were ligated. The generated plasmid pY-Cterm encoded residues 70−146 of yeast CaM. The nucleotide sequence was confirmed using a Hitachi model SQ5500 DNA autosequencer.

*Protein Purification.* Scallop CaM was prepared according to the methods of Yazawa et al. (*32*). Fragments F12 and F34 corresponding to the N-terminal (residues 1−75) and the C-terminal halves (residues 78−148), respectively, of scallop CaM were prepared by tryptic digestion (*25*).

The recombinant proteins of yeast CaM (YCM0) and its deletion mutants YCMΔ (residues 1−132 with an extra residue Ile130) and Y12 (residues 1−77) were expressed in *E. coli* TG1 and purified as described previously (*5*, *11*, *30*). The C-terminal half of yeast CaM, Y34 (residues 70−146), encoded by plasmid pY-Cterm was expressed similarly and purified as follows. Chromatography on phenyl Sepharose CL-4B was performed in a manner similar to that for Y12 (*30*) except that the concentration of ammonium sulfate in the washing buffer (1 column volume) and in the elution buffer was 0.6 M instead of 0.4 M. The fractions containing Y34 were collected and concentrated by the trichloroacetic acid precipitation method (*32*). The protein solution was desalted by gel filtration (Sephadex G-25) and loaded onto a column of DEAE Cellulofine A500 (50 mL bed) equilibrated with 10 mM Tris, 10 mM imidazole hydrochloride (pH 6.8), and 0.1 mM EGTA containing 0.05 M NaCl. The column was washed with 4 column volumes of the equilibration buffer, and then the adsorbed proteins were eluted by a linear gradient of the concentration of NaCl to 0.2 M in the equilibration buffer. Y34 was eluted at 0.12 M NaCl with a purity of the apparent single band on PAGE. Contaminating $Ca^{2+}$ in the protein solution was removed as described previously (*11*). The proteins used in this work are shown schematically in Figure 1.

*$Ca^{2+}$ Binding Measurement.* The extent of $Ca^{2+}$ binding was measured by the flow dialysis method using $^{45}CaCl_2$ (DuPont-NEN) in 0.1 M NaCl and 20 mM MOPS/NaOH (pH 7.0) at 25 °C in the presence of 25−100 μM CaM or 50−200 μM fragments as described previously (*11*, *33*). For each of the protein samples, the measurements were taken

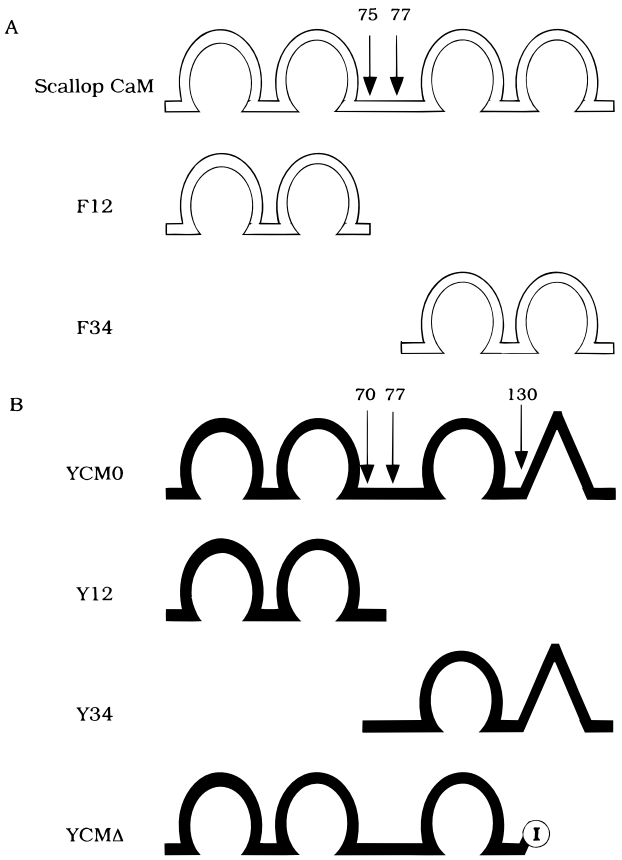


FIGURE 1: Schematic presentation of CaMs and their fragments. (A) A whole structure of the scallop CaM is shown at the top. The arrows indicate the site of trypsin digestion. The N- and the C-terminal half-molecular fragments named F12 and F34 are shown at the middle and bottom, respectively. (B) A whole structure of the yeast CaM (YCM0) is shown at the top. The arrows show the sites at which the initiation or stop codon was generated. The expressed N- and C-terminal half-molecules named Y12 and Y34 are shown in the second and third lines, respectively. Mutant YCMΔ in which the site IV sequence was deleted is shown at the bottom.

three times and all of the data points were analyzed together by fitting to Adair's equation (Figure 2); the results for YCM0 and YCMΔ were fitted to a three-site model, while the results for scallop CaM were fitted to a four-site model (*11*). The results for F12, F34, and Y12 were fitted to a two-site model:

$$y = (x/K_1 + 2x^2/K_1K_2)/(1 + x/K_1 + x^2/K_1K_2) + jx \qquad (1)$$

and the results of Y34 were fitted to a single-site model:

$$y = x/K_1/(1 + x/K_1) + jx \qquad (2)$$

where $K_1$ and $K_2$ are the macroscopic dissociation constants, $y$ is the number of bound $Ca^{2+}$ (moles per mole of protein), $x$ is the concentration of free $Ca^{2+}$, and $j$ is the slope term for nonspecific binding. Results of analyses giving an $R^2$ value of >0.997 were shown as best-fit curves.

*Circular Dichroism Spectra.* The CD spectra were measured at 25 °C with a rectangular quartz cell (1 mm light path) using a JASCO J-500A CD spectropolarimeter equipped with a DP-500N data processor. The protein concentrations were 25 (scallop CaM, YCM0, or YCMΔ) or 50 μM (F12, F34, Y12, or Y34) in 0.1 M NaCl and 20 mM MOPS/NaOH (pH 7.0) containing $CaCl_2$ at various concentrations. Mea-

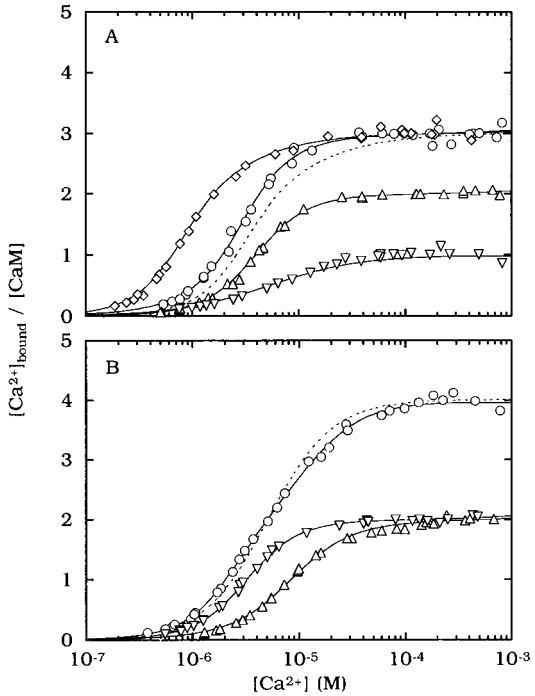


FIGURE 2: $Ca^{2+}$ binding to CaMs and fragments. The extent of $Ca^{2+}$ binding was measured by the flow dialysis method using $^{45}CaCl_2$ in a medium of 0.1 M NaCl and 20 mM MOPS/NaOH at pH 7.0 and 25 °C: (A) (○) YCM0, (△) Y12, (▽) Y34, and (◇) YCMΔ and (B) (○) scallop CaM, (△) F12, and (▽) F34. Solid lines show the best-fit curves to Adair's equation (Materials and Methods) for each set of data. The dotted line represents the sum of the $Ca^{2+}$ binding curves of Y12 and Y34 (A) or F12 and F34 (B).

surements on the equimolar mixture were performed in the presence of each of the half-molecular fragments at 25 $\mu$M. The spectra were scanned 16 times on each sample for the data processing, and the values of mean residue CD at 222 nm [$-\Delta\epsilon_{222}$ ($cm^{-1}$ $M^{-1}$)] were determined. The two independent measurements were performed for each sample, and all of the data points were used for analysis (Figure 3).

*$^1$H NMR Spectra.* NMR signals of the C2 protons of His residues (a) and the lower-field-shifted amide protons (b) were monitored using a JEOL JNM-A600 spectrometer at $^1$H frequencies of 600 MHz. The experimental conditions were as follows: (a) 0.8 mM protein, 50 mM KCl, and 10 mM MOPS/KOD (pH 7.5) in $D_2O$ and (b) 1.6 mM protein and 50 mM KCl in $H_2O$ containing 10% $D_2O$ and pH adjusted to 7.2−7.7 by addition of KOD. The NMR spectra of these samples were observed at various concentrations of $Ca^{2+}$. The FID data were recorded with 8192 complex data points over a frequency width of 8000 Hz. Water peak suppression was achieved by the 1-1 echo method. Chemical shifts are reported in parts per million relative to the internal standard TSP (0 ppm). The temperature of samples was kept at 30 ± 0.1 °C throughout the experiments. The NMR data processing was performed using Felix95 software (Molecular Simulations Inc., San Diego, CA) running on an SGI Indigo2 or $0_2$ workstation.

*Protein Concentration.* The protein concentration was determined by the biuret method (*34*) or by the method of Bradford (*35*) using a Bio-Rad protein assay reagent. In the latter method, each authentic protein was used as the standard which was determined by the biuret method using bovine serum albumin as a standard.

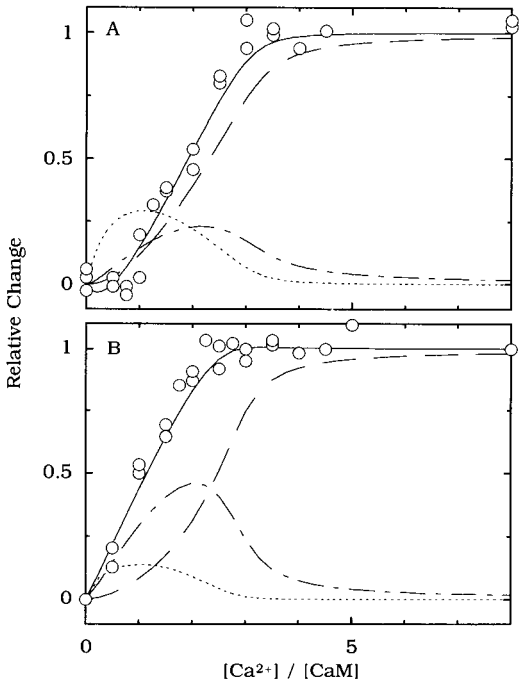


FIGURE 3: Effect of total $Ca^{2+}$ concentration on the CD spectral changes of YCM0 (A) and YCMΔ (B). Relative changes in $\Delta\epsilon_{222}$ (○) were calculated, and they were compared with the statistical distributions of $P_{Ca-CaM}$ (dotted line), $P_{Ca_2-CaM}$ (dotted-dashed line), and $P_{Ca_3-CaM}$ (dashed line). These lines were calculated from eqs 3−7 (Materials and Methods), using the macroscopic dissociation constants given in Table 1 and the total concentration of YCM0 or YCMΔ ($P_0$ = 25 $\mu$M). Solid lines were the best-fit curves based on eq 8.

*Computer Simulation.* The $Ca^{2+}$ dependence of CD and NMR spectral changes of YCM0 and YCMΔ was analyzed by estimating the relative contribution of the $Ca^{2+}$-bound species, Ca−CaM, $Ca_2$−CaM, and $Ca_3$−CaM. For calculating the relative distribution of each species, the concentration of free $Ca^{2+}$, $Ca_f$, was first estimated from eq 3:

$$Ca_0/P_0 = [(Ca_f/P_0)(1 + Ca_f/K_1 + Ca_f^2/K_1K_2 + Ca_f^3/K_1K_2K_3) + Ca_f/K_1 + 2Ca_f^2/K_1K_2 + 3Ca_f^3/K_1K_2K_3]/(1 + Ca_f/K_1 + Ca_f^2/K_1K_2 + Ca_f^3/K_1K_2K_3) \quad (3)$$

where $P_0$ and $Ca_0$ are the concentrations of total CaM and $Ca^{2+}$, respectively, and $K_1$, $K_2$, and $K_3$ are the macroscopic dissociation constants determined by the $Ca^{2+}$ binding measurements. Values of $Ca_f$ giving the $Ca_0/P_0$ values converging within 0.001% deviations were estimated. Then the concentration of free CaM, $P_f$, is given by eq 4.

$$P_f = P_0/(1 + Ca_f/K_1 + Ca_f^2/K_1K_2 + Ca_f^3/K_1K_2K_3) \quad (4)$$

The $Ca^{2+}$-dependent distribution of each species, that is, $P_{Ca-CaM}$, $P_{Ca_2-CaM}$, and $P_{Ca_3-CaM}$ can be calculated as follows:

$$P_{Ca-CaM} = Ca_fP_f/K_1 \quad (5)$$

$$P_{Ca_2-CaM} = Ca_f^2P_f/K_1K_2 \quad (6)$$

$$P_{Ca_3-CaM} = Ca_f^3P_f/K_1K_2K_3 \quad (7)$$

Using these values, the $Ca^{2+}$ dependence of the CD spectral

Table 1: $Ca^{2+}$ Binding to CaM and Fragments[a]

| CaM | $K_1$ ($\mu$M)[b] | $K_2$ ($\mu$M)[b] | $K_3$ ($\mu$M)[b] | $K_4$ ($\mu$M)[b] | $j$ |
|---|---|---|---|---|---|
| YCM0 | 2.8(0.8) | 3.6(2.0) | 2.2(0.9) | | 31.4 |
| Y12 | 13(2) | 1.2(0.2) | | | 26.6 |
| Y34 | 5.2(0.4) | | | | −16.5 |
| YCMΔ | 2.2(1.1) | 0.30(0.17) | 2.2(0.5) | | 55.6 |
| scallop CaM | 7.8(3.9) | 0.68(0.39) | 21(8) | 7.7(2.5) | −39.7 |
| F12 | 12(1) | 5.8(0.6) | | | 23.5 |
| F34 | 12(2) | 0.85(0.13) | | | 67.7 |

[a] Each set of macroscopic dissociation constants $K_1$, $K_2$, $K_3$, and $K_4$ gives the corresponding best-fit curve to Adair's equation (Materials and Methods) shown in Figure 2. [b] Standard errors for the evaluated dissociation constants are indicated in parentheses.

changes is given by eq 8:

$$y = \alpha P_{Ca-CaM} + \beta P_{Ca_2-CaM} + P_{Ca_3-CaM} \quad (8)$$

where $y$ is the relative spectral change and $\alpha$ and $\beta$ are the contribution factors of Ca−CaM and $Ca_2$−CaM, respectively, with respect to the spectral change of the final $Ca^{2+}$-saturated conformation. The contribution factors, $\alpha$ and $\beta$, were estimated by curve fitting. The $Ca^{2+}$ dependence of the NMR spectral changes was analyzed similarly. The whole process of the analysis was performed with a program written in Think C.

## RESULTS

*$Ca^{2+}$ Binding.* The results of $Ca^{2+}$ binding measurement are summarized in Figure 2, and macroscopic dissociation constants satisfying Adair's equation (Materials and Methods) are summarized in Table 1. The half-molecular fragment Y12 bound 2 mol of $Ca^{2+}$, while Y34 containing the sequence of sites III and IV of yeast CaM bound 1 mol of $Ca^{2+}$ (Figure 2). Judging from their $Ca^{2+}$ binding curves, the N-domain of YCM0 is probably occupied first by $Ca^{2+}$ (*29*; S.-y. Ohki et al., unpublished results) in contrast to the results for scallop or vertebrate CaM of which the C-domain is occupied first (*25*, *36*) (Figure 2). Fragment Y12 showed a highly cooperative $Ca^{2+}$ binding as does the C-domain of scallop CaM as evidenced by the significantly lower value of $K_2$ compared with $K_1$ (Table 1). Compared with the sum of the $Ca^{2+}$ binding curves of each half-molecular fragment, Y12 and Y34, the $Ca^{2+}$ binding to the three sites in YCM0 is highly cooperative, giving a steeper curve with a midpoint at lower $Ca^{2+}$ concentrations than the sum (Figure 2A), while the sum of two fragments from scallop CaM fitted well to those of intact CaM as described previously (Figure 2B) (*25*). YCMΔ bound three $Ca^{2+}$ and showed an affinity for $Ca^{2+}$ remarkably higher than those of the half-molecular fragments, Y12 and Y34, and their sum, despite its lack of C-terminal residues (Figure 2A) (*5*). Quantitative analysis of these properties (Table 1) clearly indicated that the two half-molecular domains of yeast CaM interact with each other to modulate the $Ca^{2+}$ affinity.

*Circular Dichroism Spectra.* The $Ca^{2+}$-dependent conformational changes of CaMs and fragments were studied with far-UV CD spectroscopy. Values of $-\Delta\epsilon_{222}$ were calculated from the spectra in the presence of 0.2 mM $CaCl_2$ (with $Ca^{2+}$) or 0.1 mM EGTA (without $Ca^{2+}$), and they are summarized in Table 2. In contrast to the apparent $Ca^{2+}$-dependent increase in $-\Delta\epsilon_{222}$ observed for scallop or vertebrate CaM, YCM0 showed a $Ca^{2+}$-dependent decrease in $-\Delta\epsilon_{222}$ (Table 2) (*5*, *7*). If the $Ca^{2+}$-dependent decrease in $-\Delta\epsilon_{222}$ is considered, YCM0 in the $Ca^{2+}$-free conformation is apparently more helical than in the $Ca^{2+}$-saturated conformation. Each of the half-molecular fragments of yeast CaM, that is, Y12 and Y34, and YCMΔ which lacked the site IV sequence, however, showed an apparent increase in α-helicity as a result of $Ca^{2+}$ binding (Table 2). The equimolar mixture of Y12 and Y34 also showed the $Ca^{2+}$-dependent increase in α-helicity, and the $Ca^{2+}$ dependence of $-\Delta\epsilon_{222}$ was similar to that for scallop CaM (Table 2).

Table 2: $Ca^{2+}$-Induced CD Spectral Change[a]

| CaM | $-\Delta\epsilon_{222}$ ($M^{-1}$ $cm^{-1}$) without $Ca^{2+}$ | $-\Delta\epsilon_{222}$ ($M^{-1}$ $cm^{-1}$) with $Ca^{2+}$ | $Ca^{2+}$-induced change |
|---|---|---|---|
| YCM0 | 4.43 | 3.95 | −0.48 |
| YCMΔ | 3.61 | 4.19 | 0.58 |
| Y12 | 4.55 | 5.53 | 0.98 |
| Y34 | 4.04 | 4.70 | 0.66 |
| Y12 and Y34 | 4.21 | 5.18 | 0.97 |
| Y12 and Y34[b] | 4.29 | 5.12 | 0.83 |
| scallop CaM | 4.14 | 5.03 | 0.89 |
| F12 | 3.69 | 4.42 | 0.73 |
| F34 | 4.20 | 5.45 | 1.25 |
| F12 and F34[b] | 3.96 | 4.96 | 1.00 |

[a] CD spectra were measured under the following conditions: 0.1 M NaCl, 20 mM MOPS/NaOH (pH 7.0), and 0.1 mM EGTA (without $Ca^{2+}$) or 0.2 mM $CaCl_2$ (with $Ca^{2+}$) at 25 °C. [b] The values were calculated using the data of each half-fragment.

In the course of $Ca^{2+}$ titration of proteins other than YCM0 and YCMΔ, $-\Delta\epsilon_{222}$ increased almost linearly with increases in the molar ratio of $Ca^{2+}$:protein up to their $Ca^{2+}$ binding capacity, and then the increase leveled off. Similarly, addition of $Ca^{2+}$ to an equimolar mixture of Y12 and Y34 caused an increase in $-\Delta\epsilon_{222}$ almost linearly up to 3 equiv of $Ca^{2+}$ with respect to Y12 or Y34 (data not shown). As shown in Figure 3 by the relative spectral changes, effects of $Ca^{2+}$ on $-\Delta\epsilon_{222}$ of YCM0 and YCMΔ are different from the one of the equimolar mixture. Major conformational changes of YCM0 and YCMΔ occurred after addition of 1−3 and 0−2 equiv of $Ca^{2+}$, respectively (Figure 3), and YCM0 showed decrease in $-\Delta\epsilon_{222}$, in contrast to the $Ca^{2+}$-dependent increase observed in other cases (Table 2). The results suggest that the N- and the C-terminal domains in YCM0 and YCMΔ interact with each other.

*Estimation of Intermediate Species and Their Contribution to the CD Changes.* The relative change in $-\Delta\epsilon_{222}$ was analyzed according to eq 8 (Figure 3) on the basis of the $Ca^{2+}$-dependent distributions of Ca−CaM, $Ca_2$−CaM, and $Ca_3$−CaM (Figure 3). Since YCM0 binds all three $Ca^{2+}$ in a highly cooperative manner (Table 1), only small peaks in the distribution of Ca−CaM and $Ca_2$−CaM appeared one by one, and then the most stable $Ca^{2+}$-saturated form, $Ca_3$−CaM, appeared with increases in the concentration of $Ca^{2+}$ (Figure 3A). On the other hand, YCMΔ has two high-affinity $Ca^{2+}$ binding sites with high cooperativity and a low-affinity $Ca^{2+}$ binding site (Table 1). As a result, a small peak in the distribution of Ca−CaM and a larger peak of $Ca_2$−CaM appeared clearly (Figure 3B), and then $Ca_3$−CaM was formed.

The contribution factors $\alpha$ and $\beta$ of eq 8 which give the best-fit curves (solid lines in Figure 3) to the data were −0.39 and 1.00, respectively, for YCM0, and 0.35 and 1.05, respectively, for YCMΔ. These results indicate that saturation

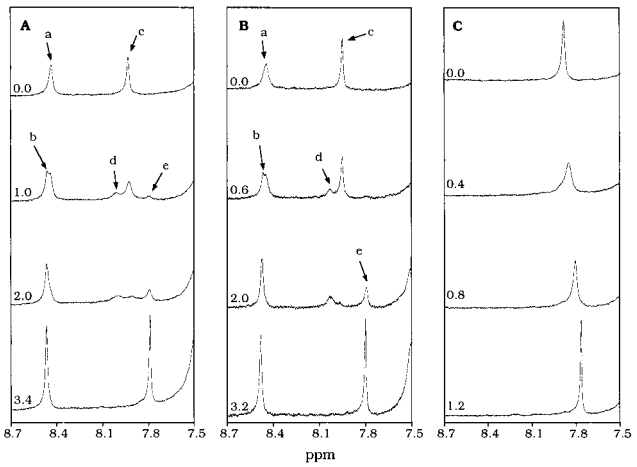


FIGURE 4: $Ca^{2+}$ dependence of $^1H$ NMR spectra around the C2 proton signals of His residues: (A) YCM0, (B) YCMΔ, and (C) Y34. Peaks a and b arise from His61 in the N-domain, and peaks c−e arise from His107 in the C-domain. The spectra were measured in a medium of 50 mM KCl and 50 mM MOPS/KOD at pH 7.5 and 30 °C. The protein concentration was 0.8 mM. Added $Ca^{2+}$:protein molar ratios are indicated in each panel.

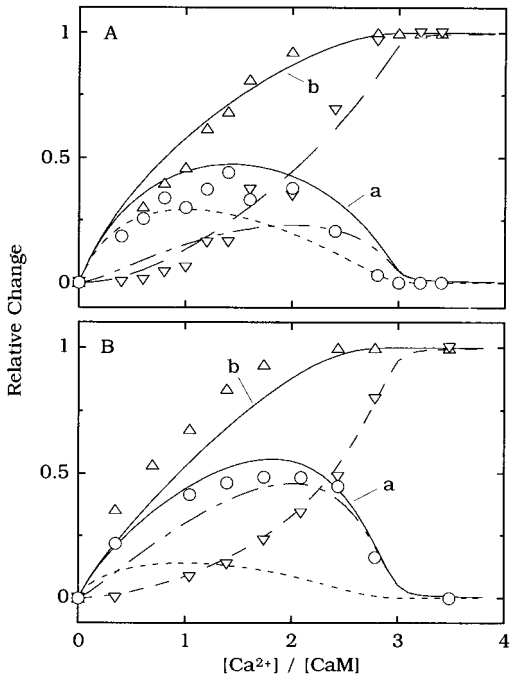


FIGURE 5: Effect of total $Ca^{2+}$ concentration on the NMR spectral changes of YCM0 (A) and YCMΔ (B). Relative changes in the signal intensities of His61-C2H (△, peak b in Figure 4) and His107-C2H (○, peak d; and ▽, peak e; each in Figure 4) were compared with the statistical distributions of $P_{Ca-CaM}$ (dotted line), $P_{Ca_2-CaM}$ (dotted-dashed line), and $P_{Ca_3-CaM}$ (dashed line). These lines were calculated according to eqs 3−7 (Materials and Methods). Solid lines a and b represent traces for $P_{Ca-CaM} + P_{Ca_2-CaM}$, and $P_{Ca-CaM} + P_{Ca_2-CaM} + P_{Ca_3-CaM}$, respectively.

of two out of three $Ca^{2+}$-binding sites is sufficient to complete the overall $Ca^{2+}$-saturated conformation of YCM0 and YCMΔ.

*$^1H$ NMR Spectra.* Yeast CaM contains a single His residue in each half-molecular domain: His61 in site II in the N-domain and His107 at the linker between site III and site IV in the C-domain. $^1H$ NMR spectra of YCM0, YCMΔ, and Y34 in the regions of the C2 proton signals of His are shown in Figure 4. A signal from His61 (peak a) appeared at 8.43 ppm in the $Ca^{2+}$-free state of YCM0 and YCMΔ. This peak progressively diminished in intensity with increases in the concentration of $Ca^{2+}$, and a new peak at 8.46 ppm (peak b) corresponding to the $Ca^{2+}$-saturated conformation appeared in a slow-exchange manner. Therefore, the local conformation of the N-domain around His61 seems similar in these two molecules. On the other hand, the signals from His107 showed three different peaks depending on the concentration of $Ca^{2+}$. In YCM0, a signal (peak c) appeared at 7.91 ppm in the absence of $Ca^{2+}$. It shifted first downfield (peak d, 7.99 ppm) in a slow-exchange manner and then upfield with increases in the concentration of $Ca^{2+}$. The latter signal (peak e) was observed at 7.78 ppm (Figure 4A). Three similar peaks were observed in YCMΔ (Figure 4B). Therefore, His107 in the C-domain of these two molecules experiences three different conformational states with increases in the concentration of $Ca^{2+}$: the apo state (peak c), the intermediate state (peak d), and the $Ca^{2+}$-saturated state (peak e).

The $Ca^{2+}$ dependence of the His107 signals in the isolated C-domain, Y34, was also examined (Figure 4C). The peak appeared at 7.87 ppm in the absence of $Ca^{2+}$ shifted upfield in a fast-exchange manner with increases in $Ca^{2+}$ concentration, and finally appeared at 7.76 ppm in the $Ca^{2+}$-saturated state. The exchange behavior of His107 in the isolated C-domain is different from that in the intact yeast CaM (Figure 4). A similar result has been observed by Starovasnik et al. (*29*), indicating a possible interdomain interaction. Therefore, the intermediate peak (peak d) of YCM0 and YCMΔ detected in our experiments can be assigned to a species with the $Ca^{2+}$-saturated N-domain, and the peak in the $Ca^{2+}$-saturated state (peak e) may correspond to the conformation of the species with the $Ca^{2+}$-saturated C-domain of YCM0 and YCMΔ.

The $Ca^{2+}$ dependence of the intensity of these His signals from YCM0 or YCMΔ was analyzed on the basis of the distribution of each species ($P_{Ca-CaM}$, $P_{Ca_2-CaM}$, and $P_{Ca_3-CaM}$) which was calculated as described previously by using macroscopic dissociation constants (Table 1) and the concentration of total protein, $P_0 = 0.8$ mM (Figure 5). The $Ca^{2+}$ dependence of these values together with the sum of $P_{Ca-CaM}$ and $P_{Ca_2-CaM}$ (solid line a) and the sum of $P_{Ca-CaM}$, $P_{Ca_2-CaM}$, and $P_{Ca_3-CaM}$ (solid line b) is shown in Figure 5. The $Ca^{2+}$-dependent changes in intensity of His61 in the $Ca^{2+}$-saturated state (peak b in Figure 4), His107 in the $Ca^{2+}$-saturated state (peak e in Figure 4), and His107 in the intermediate state (peak d in Figure 4) are similar to those of curve b, the curve for $P_{Ca_3-CaM}$ (broken line), and curve a, respectively (Figure 5). Therefore, the $Ca^{2+}$ affinity of site III is the lowest among the three sites in YCM0 and YCMΔ. The conformation of the C-domain, especially around His107, is not independent of the N-domain and is influenced by at least 1 mol of $Ca^{2+}$ binding to the N-domain.

*Hydrogen Bonds.* Figure 6 shows $^1H$ NMR spectra of YCM0 and YCMΔ in the region of lower-field-shifted amide proton signals. Signals of Gly25, His61, and Gly98 (at 10.75, 10.33, and 10.03 ppm, respectively) were observed in the $Ca^{2+}$-saturated state. These are lower-field-shifted due to strong hydrogen bonding to the side chain carboxylate oxygen of the Asp residue five residues ahead in each of the three EF-hand $Ca^{2+}$ binding loops (*29*, *30*). In the spectrum of the apo YCM0, a broad peak assigned to Gly25

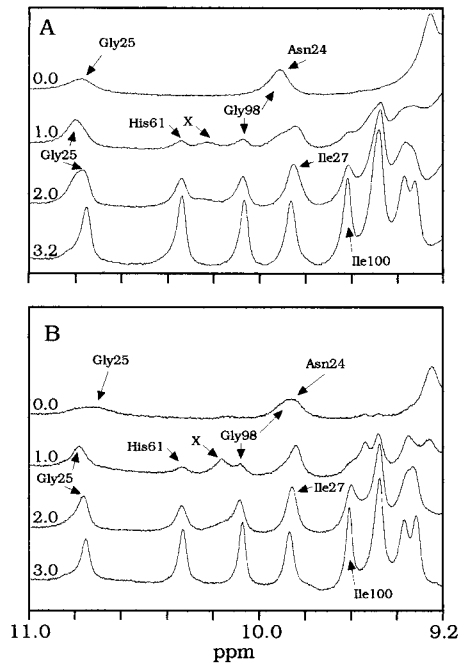


FIGURE 6: $^1$H NMR spectra around signals of amide protons constituting the $Ca^{2+}$ binding loops. Spectra of YCM0 (A) and YCMΔ (B) are shown in each panel. Assignments of several signals and $Ca^{2+}$:protein molar ratios are shown in each panel. Peak x has not been assigned yet.

was observed around 10.7 ppm. With increases in the concentration of $Ca^{2+}$, this broad peak shifted to a lower field, and then the His61 peak appeared, which was accompanied by the appearance of the Gly98 peak (Figure 6A). At the same time, the signal of Gly25 shifted upfield in a slow-exchange manner. Similar results were obtained in the $Ca^{2+}$ titration of YCMΔ (Figure 6B), except that the upfield shift of Gly25 occurred in a fast-exchange manner. In the $Ca^{2+}$ titration of Y12, however, the upfield shift of the Gly25 signal was not observed (data not shown), in which the spectra in the apo and the $Ca^{2+}$-saturated state shown by Starovasnik et al. (*29*) were confirmed (data not shown). These results suggest a $Ca^{2+}$-dependent interdomain interaction, such as hydrogen bond formation in site III (Gly98···Asp93) accompanied by $Ca^{2+}$ binding and hydrogen bond formation in site II (His61···Asp56). Similarly, the upfield shift of the Gly25 signal in site I and another transiently appearing signal (peak x in Figure 6), which has not been assigned yet, are notable and may provide further evidence for the interdomain interaction accompanying the cooperative $Ca^{2+}$ binding.

## DISCUSSION

Yeast CaM binds three $Ca^{2+}$ in a cooperative manner (Figure 2A and Table 1) (*6*, *11*, *29*). The possible interaction between the two half-molecular domains in yeast CaM is suggested by comparing the $Ca^{2+}$ binding properties (Table 1 and Figure 2), the $Ca^{2+}$-induced CD spectral changes (Table 2), and the $Ca^{2+}$ dependence of several $^1$H NMR signals (Figures 4 and 6) (*29*) of the intact yeast CaM, YCMΔ, and half-molecules Y12 and Y34. As fragment YCMΔ with a deletion of the 17 C-terminal residues showed properties (Figure 2 and Tables 1 and 2) different from those of YCM0 as well as those of the half-molecular fragments, the C-terminal sequence missing in YCMΔ probably plays a role in communication between the two domains collaborating with a sequence extended to site III. Since the N-terminal domain is the high-affinity $Ca^{2+}$ binding site of yeast CaM (Figure 2 and Table 1) (*29*; S. Ohki et al., unpublished results), $Ca^{2+}$ binding to the N-domain may induce some conformational change in the C-domain through the C-terminal sequence which may be responsible for the cooperative $Ca^{2+}$ binding. Most probably, the defective site IV sequence of YCM0 makes contact with the N-domain, and then the cooperative $Ca^{2+}$ binding may occur.

Quantitative analyses of the $Ca^{2+}$ dependences of CD (Figure 3) and $^1$H NMR (Figure 5) spectra provided the detail of the interdomain interaction in yeast CaM. The results of $Ca^{2+}$ titration of the lower-field-shifted amide protons in each $Ca^{2+}$ binding loop are consistent with these results (Figure 6). As the contribution of $Ca_2$−CaM to the final CD spectral change was equal to that of $Ca_3$−CaM ($\beta = 1.00$), the overall $Ca^{2+}$-saturated structure of YCM0 or YCMΔ, including the conformational change in the C-domain, can be completed when the N-domain is saturated with $Ca^{2+}$ (Figure 3). Since the apparent $Ca^{2+}$-dependent increase in α-helicity of CaM is thought of as a result of some structural reorientation of the α-helical segments (*37*), the apparent decrease in α-helicity specific to YCM0 and yeast CaM would indicate a different way of rearrangement in the secondary structure which leads to the interdomain interaction responsible for the highly cooperative $Ca^{2+}$ binding.

The $Ca^{2+}$ dependence of the C2 proton of His107 in the C-domain of YCM0 and YCMΔ showed the three-state spectral changes, which was different from that in Y34 exhibiting only the upfield shift (Figure 4). The result shown in Figure 5 indicated that the upfield shift of His107 peak may result from $Ca^{2+}$ binding to the C-domain, while the downfield shift observed on binding of the initial two $Ca^{2+}$ may result from $Ca^{2+}$ binding to the N-domain. Therefore, His107 is sensitive to the interdomain cross-talk. Another residue detected as a transiently observed $^1$H NMR signal (peak x in Figure 6), as well as Gly25 which showed the upfield shift of the amide proton signal (Figure 6), may also be involved. The interaction accompanies the highly cooperative binding of the three $Ca^{2+}$ in YCM0 (Figure 2 and Table 1), while the same interaction lacking the 17 most C-terminal residues caused different effects in YCMΔ on the exchange rate of the amide proton of Gly25 (Figure 6) and emphasized the cooperative $Ca^{2+}$ binding in the N-domain of YCMΔ (Figure 2 and Table 1). The 17 residues in site IV may be responsible for the observed positive cooperativity in yeast CaM which may result from the interaction between the N-domain and $Ca^{2+}$ binding site III.

The interdomain interaction observed in yeast CaM, which might also be responsible for the characteristic structure observed by solution X-ray scattering (*31*), is unusual, since vertebrate or invertebrate CaM takes the dumbbell shape and the interdomain interaction is stable only in the ternary complex formed with the target peptide (*31*, *33*). These properties of yeast CaM suggest an unusual mode of target recognition which is different from the typical one of vertebrate CaM.

Among the atomic structures of the EF-hand $Ca^{2+}$ binding proteins (*19*−*21*, *38*−*42*), those of amphioxus sarcoplasmic $Ca^{2+}$ binding protein (*42*) and recoverin (*39*) are interesting when considering the interdomain interaction of yeast CaM. Although they consist of four EF-hand motifs, site IV in their

C-terminal half-domains does not bind $Ca^{2+}$. Despite the defect in site IV, the two EF-hand motifs in the C-domain maintain the apparent 2-fold rotation symmetry, and interact with the N-domain. Since Y34 showed high affinity for a single $Ca^{2+}$, similar symmetry may also be maintained in yeast CaM. In recoverin, part of the site III sequence makes contact with site II and the C-terminal segment of the site IV sequence interacts with the N-terminal half molecular domain. As a result, a hydrophobic face is formed on the other side of the molecule relative to the four $Ca^{2+}$ binding loops (*39*), which might be responsible for interaction with targets. A similar structure is observed in calcineurin B, another member consisiting of four EF-hand motifs, in which the hydrophobic face makes contact with the helical segment of the catalytic subunit (*41*). In yeast CaM, the C-terminal sequence and a part of the site III sequence may work similarly in recognizing target proteins, since Matsuura et al. (*5*) showed that YCMΔ could not activate the phosphodiesterase and myosin light chain kinase of vertebrates at all. The difference in the mechanism for target recognition may be one of the major reasons for the observed poor activation by yeast CaM of target enzymes isolated from vertebrate. If this is the case, target proteins isolated from yeast may be more efficiently activated by yeast CaM than by vertebrate CaM.

When each of the N- and the C-terminal half-molecule of yeast CaM was overexpressed in yeast cells, the essential function of the intact molecule was complemented (*12*). Although each half-molecule of CaM appears to work as the smallest functional unit, clear differences between the whole molecule and the half-molecular fragments were shown. This study provides evidence that the N- and the C-terminal domains in yeast CaM interact with each other, which influenced the $Ca^{2+}$ binding property of the whole molecule. In vertebrate CaM, this kind of interdomain interaction is found in the presence of target proteins or under conditions of low ionic strength (*33*, *44*, *45*). The site IV sequence in yeast CaM is important for maintaining the interaction, and may have a specific role in recognizing target proteins. A further study using isolated target proteins from yeast cells and a three-dimensional structural analysis of yeast CaM is in progress.

## REFERENCES


1. Kretsinger, R. H., and Nockolds, C. E. (1973) *J. Biol. Chem. 248*, 3313−3326.
2. Klee, C. B., and Vanamann, T. C. (1982) *Adv. Protein Chem. 35*, 213−321.
3. Toda, H., Yazawa, M., Sakiyama, F., and Yagi, K. (1985) *J. Biochem. 98*, 833−842.
4. Davis, T. N., Urdea, M. S., Masiarz, F. R., and Thorner, J. (1986) *Cell 47*, 423−431.
5. Matsuura, I., Ishihara, K., Nakai, Y., Yazawa, M., Toda, H., and Yagi, K. (1991) *J. Biochem. 109*, 190−197.
6. Luan, Y., Matsuura, I., Yazawa, M., Nakamura, T., and Yagi, K. (1987) *J. Biochem. 102*, 1531−1537.
7. Ohya, Y., Uno, I., Ishikawa, T., and Anraku, Y. (1987) *Eur. J. Biochem. 168*, 13−19.
8. Matsuura, I., Kimura, E., Tai, K., and Yazawa, M. (1993) *J. Biol. Chem. 268*, 13267−13273.
9. Lukas, T. J., Colinge, M., Heiech, J., and Watterson, D. M (1994) *Biochim. Biophys. Acta 1223*, 341−347.
10. Kimura, E., Matsuura, I., Tai, K., Nakashima, K., and Yazawa, M. (1995) *Proc. Jpn. Acad. 71B*, 293−298.
11. Nakashima, K., Maekawa, H., and Yazawa, M. (1996) *Biochemistry 35*, 5602−5610.
12. Sun, G. H., Ohya, Y., and Anraku, Y. (1991) *J. Biol. Chem. 266*, 7008−7015.
13. Ikura, M. (1996) *Trends Biochem. Sci. 21*, 14−17.
14. Barbato, G., Ikura, M., Kay, L. E., Pastor, R. W., and Bax, A. (1992) *Biochemistry 31*, 5269−5278.
15. Tjandra, N., Kuboniwa, H., Ren, H., and Bax, A. (1995) *Eur. J. Biochem. 230*, 1014−1024.
16. Babu, Y. S., Bugg, C. E., and Cook, W. J. (1988) *J. Mol. Biol. 204*, 191−204.
17. Zhang, M., Tanaka, T., and Ikura, M. (1995) *Nat. Struct. Biol. 2*, 758−767.
18. Kuboniwa, H., Tjandra, N., Grzesiek, S., Ren, H., Klee, C. B., and Bax, A. (1995) *Nat. Struct. Biol. 2*, 768−776.
19. Ikura, M., Clore, G. M., Gronenborn, A. M., Zhu, G., Klee, C. B., and Bax, A. (1992) *Science 256*, 632−638.
20. Meador, W. E., Means, A. R., and Quiocho, F. A. (1992) *Science 257*, 1251−1255.
21. Meador, W. E., Means, A. R., and Quiocho, F. A. (1993) *Science 262*, 1718−1721.
22. Walsh, M., Stevens, F. C., Kuznicki, J., and Drabikowski, W. (1977) *J. Biol. Chem. 252*, 7440−7443.
23. Drabikowski, W., Kuznicki, J., and Grabarek, Z. (1977) *Biochim. Biophys. Acta 485*, 124−133.
24. Drabikowski, W., Brzeska, H., and Venyaminov, S. Y. (1982) *J. Biol. Chem. 257*, 11584−11590.
25. Minowa, O., and Yagi, K. (1984) *J. Biochem. 96*, 1175−1182.
26. Vogel, H. J., Lindahl, L., and Thulin, E. (1983) *FEBS Lett. 157*, 241−246.
27. Brzeska, H., Szynkiewicz, J., and Drabikowski, W. (1983) *Biochem. Biophys. Res. Commun. 115*, 87−93.
28. Brockerhoff, S. E., Edmonds, C. G., and Davis, T. N. (1992) *Protein Sci. 1*, 504−516.
29. Starovasnik, M. A., Davis, T. N., and Klevit, R. E. (1993) *Biochemistry 32*, 3261−3270.
30. Ohki, S., Miura, K., Saito, M., Nakashima, K., Maekawa, H., Yazawa, M., Tsuda, S., and Hikichi, K. (1996) *J. Biochem. 119*, 1045−1055.
31. Yoshino, H., Izumi, Y., Sakai, K., Takezawa, H., Matsuura, I., Maekawa, H., and Yazawa, M. (1996) *Biochemistry 35*, 2388−2393.
32. Yazawa, M., Sakuma, M., and Yagi, K. (1980) *J. Biochem. 87*, 1313−1320.
33. Yazawa, M., Vorherr, T., James, P., Carafoli, E., and Yagi, K. (1992) *Biochemistry 31*, 3171−3176.
34. Kabat, E. A., and Mayer, M. M. (1961) in *Experimental Immunology*, pp 559−560, Charles C. Thomas Publisher, Springfield, IL.
35. Bradford, M. M. (1976) *Anal. Biochem. 72*, 248−254.
36. Ikura, M., Hiraoki, T., Hikichi, K., Minowa, O., Yamaguchi, H., Yazawa, M., and Yagi, K. (1984) *Biochemistry 23*, 3124−3128.
37. Hennessey, J. P., Jr., Manavalan, P., Johnson, W. C., Jr., Malencik, D. A., Anderson, S. R., Schimerlik, M. I., and Shalitin, Y. (1987) *Biopolymers 26*, 561−571.
38. Strynadka, N. C. J., and James, M. N. G. (1989) *Annu. Rev. Biochem. 58*, 951−998.
39. Flaherty, K. M., Zozulya, S., Stryer, L., and McKay, D. B. (1993) *Cell 75*, 709−716.
40. Rayment, I., Rypniewski, W. R., Schmidt-Bäse, K., Smith, R., Tomchick, D. R., Benning, M. M., Winkelmann, D. A., Wesenberg, G., and Holden, H. M. (1993) *Science 261*, 50−58.
41. Griffith, J. P., Kim, J. L., Kim, E. E., Sintchak, M. D., Thomson, J. A., Fitzgibbon, M. J., Fleming, M. A., Caron, P. R., Hsiao, K., and Navia, M. A. (1995) *Cell 82*, 507−522.
42. Houdusse, A., and Cohen, C. (1995) *Proc. Natl. Acad. Sci. U.S.A. 92*, 10644−10647.
43. Cook, W. J., Jeffrey, L. C., Cox, J. A., and Vijay-Kumar, S. (1993) *J. Mol. Biol. 229*, 461−471.
44. Yazawa, M., Ikura, M., Hikichi, K., Luan, Y., and Yagi, K. (1987) *J. Biol. Chem. 262*, 10951−10954.
45. Yazawa, M., Matsuzawa, F., and Yagi, K. (1990) *J. Biochem. 107*, 287−291.


BI982067T